



ANTIDIABETIC ACTIVITY OF NIGELLA SATIVA (BLACK SEED)- BY MOLECULAR MODELING ELUCIDATION, MOLECULAR DYNAMIC, AND CONCEPTUAL DFT INVESTIGATION

Fouzia Mesli^{1,2*}, Ismail Daoud^{2,3}, Said Ghalem^{1,2}

1. Department of Chemistry, Abu-Bakr Belkaid University of Tlemcen, 13000, Algeria
2. Laboratory of Natural Products and Bioactive- Lasnabio, Tlemcen, 13000, Algeria
3. Department of Matter Sciences, Mohamed Khider University of Biskra, BP 145 RP; (07000), Algeria.

ARTICLE INFO

Received:

26 Mar 2019

Received in revised form:

25 Sep 2019

Accepted:

29 Sep 2019

Available online:

21 Oct 2019

Keywords: Molecular modeling – Diabetes (T2DM) –Nigella, MOE (Molecular Operating Environment)

ABSTRACT

Background and aim: ADMET prediction, 2D-, 3D-, and 4D-QSAR, QM/MM calculations, quantum chemical calculations, Molecular Dynamics, and Molecular Docking simulations have been covering a wide area in drug discovery. This theoretical approach enables to predict the mode of interaction of a ligand with its receptor. However, synthetic inhibitors were the most efficient ones; indeed, Gliptine is the most commercialized treatment of type 2 diabetes. On the other hand, natural inhibitors have also provided good activities via Dipeptidyl peptidase-4 (DPP-4) enzyme (p-Cymene, Thymoquinone, Carvacrol, α -Pinene, β -Pinene, Limonene). **Method:** In this work, we presented a theoretical investigation of dipeptidyl peptidase-4 enzyme inhibitors by natural inhibitors including the salvation parameter. To this, we used different molecular modeling approaches as molecular mechanics. Results: The molecular dynamics study was conducted for the best natural inhibitors obtained from the simulation of molecular docking with the lowest energy scores for ligands: Lig5, Lig3, and Lig ref. The interactions of our target and the studied inhibitors were further evaluated by using the molecular docking/dynamics simulations. A few key residues (GLU205, GLU206 and H-donor, ionic) were identified at the binding site of DPP-4. **Conclusion:** The obtained result of both methods, docking and dynamics molecular lead to the same conclusion and it was predicted that dithymoquinone (essential oil Nigella Sativa) presents better interaction of DPP-4 Enzyme in the presence of water in case of molecular dynamics and consequently can be the best inhibitor candidate to be investigated in vivo and in vitro.

Copyright © 2013 - All Rights Reserved - Pharmacophore

To Cite This Article: Mesli, F., Daoud, I., Ghalem S, (2019), "Antidiabetic Activity of Nigella sativa (Black Seed)-By Molecular Modeling Elucidation, Molecular Dynamic, and Conceptual DFT investigation", *Pharmacophore*, 10(5), 57-66.

Introduction

Nigella sativa L. (family Ranunculaceae) is an annual herbaceous plant that grows through the countries of the eastern- and southern of the Mediterranean basin to India, Pakistan, and Iran. In the ethnopharmacology of those countries, *N. sativa* seeds are utilized to treat gastrointestinal disorders as well as skin or respiratory ailments [1]. In recent years, *N. sativa* seeds have been pharmacologically investigated.

These investigations have demonstrated various activities including immunostimulant, cytotoxic, smooth muscles relaxant, hypoglycemic, CNS depressant, analgesic, anti-inflammatory, antitumor, and antibacterial activities [2, 3]. *N. sativa* seeds have therapeutic activities on the endocrine, immune, respiratory, and cardiovascular systems. Some of these effects have been mainly detected in volatile and fixed oils [4, 5].

Newly, it has been proved that studying the chemical responses of molecular systems can be correctly done using the conceptual DFT framework. There are various ways for modeling the response of a molecule using the electronic structure and DFT concepts [6]. The molecular global softness index was widely used to evaluate molecular response [7]. Interactions of the chemical ligand with the active site of the enzyme constitute a very complicated field because it describes the type of each interaction whether it be: hydrogen, steric, or hydrophobic.

This study aimed at theoretically elucidating the inhibition activity of DPP-4 by a series of natural inhibitors, i.e. Nigella derivatives (p-Cymene, Thymoquinone, Carvacrol, alpha-Pinene, beta-Pinene, Limonene) using the two simulation methods,

molecular dynamics and molecular docking. The natural inhibitors chosen for DPP-4 are given in Table 1. These results can help in the development of an effective therapeutic tool to prevent T2DM development.

Table 1: Some properties of inhibitors natural essential oil *Nigella Sativa* against Dipeptidyl peptidase-4

n	Name	IUPAC name	Pub Chem CID	Weight (g/mol)	Formula
L1	Nigellicine	3-methyl-1-oxo-6,7,8,9-tetrahydropyridazino[1,2-a]indazole-1	11402337	246.2619	C ₁₃ H ₁₄ N ₂ O ₃
L2	Nigellidine	11-(4-hydroxyphenyl)-3-methyl-6H,7H,8H,9H-10λ-pyridazino[1,2-a]indazol-10-ylum-1-olate	101253695	294.354	C ₁₈ H ₁₈ N ₂ O ₂
L3	Nigellimine	6,7-dimethoxyisoquinoline	20725	203.241	C ₁₂ H ₁₃ NO ₂
L4	Thymoquinone	2-Isopropyl-5-methylbenzo-1,4-quinone	10281	164.20	C ₁₀ H ₁₂ O ₂
L5	Dithymoquinone	Dithymoquinone; Nigellone	398941	328.408	C ₂₀ H ₂₄ O ₄
L6	Thymohydroquinone	2-methyl-5-propan-2-ylbenzene-1,4-diol	95779	166.220	C ₁₀ H ₁₄ O ₂
L7	Carvacrol	2-methyl-5-propan-2-ylphenol	10364	150.221	C ₁₀ H ₁₄ O
L8	alpha-Thujen	4-methyl-1-propan-2-ylbicyclo[3.1.0]hex-3-ene	17868	136.2380	C ₁₀ H ₁₆
L9	p-Cymen	2-(4-methylphenyl)propan-2-ol	14529	150.221	C ₁₀ H ₁₄ O

Theoretical Background and Computational Details

Preparation and optimization of enzyme and inhibitors

Step 1: The 3D structure of Dipeptidyl-peptidase was downloaded from PROTEIN DATA BANK (code: 4N8D) obtained by X-ray diffraction with resolution (1.65Å). DPP-4 crystallizes as a monomer (Figure 1) with 740 residue and 5959 atoms. The structures of inhibitors were downloaded from the PubChem database.

Step 2: The energy of the enzyme was minimized and geometry was conducted using Hamiltonian AM1 implanted in MOE software and then isolation of the active site of the enzyme (target). The most stable geometry of each molecule structure (ligand) was minimized by the same method (AM1). All simulations were run by using all explicit salvation models using TIP3P water. Figure 2 shows the enzyme's active site with the native ligand (ligand co-crystallized with the enzyme).

Step 3: The third step was positioning the ligands into the enzyme's active site using the docking module implanted in MOE software. The binding energy between ligands and targets was calculated using molecular mechanics. MOE software was used to obtain the minimized energy of ligands and their toxicity [8].

DFT calculations

The global response of a molecule via external perturbation can be explained using local and global reactivity indices defined within the conceptual density functional theory (DFT) [6, 9].

The chemical hardness (η) is an atom's capacity to receive electrons [5-7]. It is estimated by using the following equation:

$$\eta = \frac{I - A}{2}$$

According to Koopmans's theorem [10], electron affinity (A), ionization potential (I), and global hardness (η) and softness (S) can be defined with regard to the energy of the Lowest Unoccupied Molecular Orbital (LUMO) and the High Occupied Molecular Orbital (HOMO). Ionization potential (I) the energy of E_{HOMO} through the following equation:

$$I = -E_{HOMO}$$

Electron Affinity (A) is the energy of E_{LUMO} through the following equation:

$$A = -E_{LUMO}$$

The global softness (S) can be determined by:

$$S = \frac{2}{E_{LUMO} - E_{HOMO}}$$

The equilibrium geometries of neutral systems were optimized using the B3LYP/6-31G(d) computational method [11, 12]. All calculations were done using the Gaussian 09 package [13].

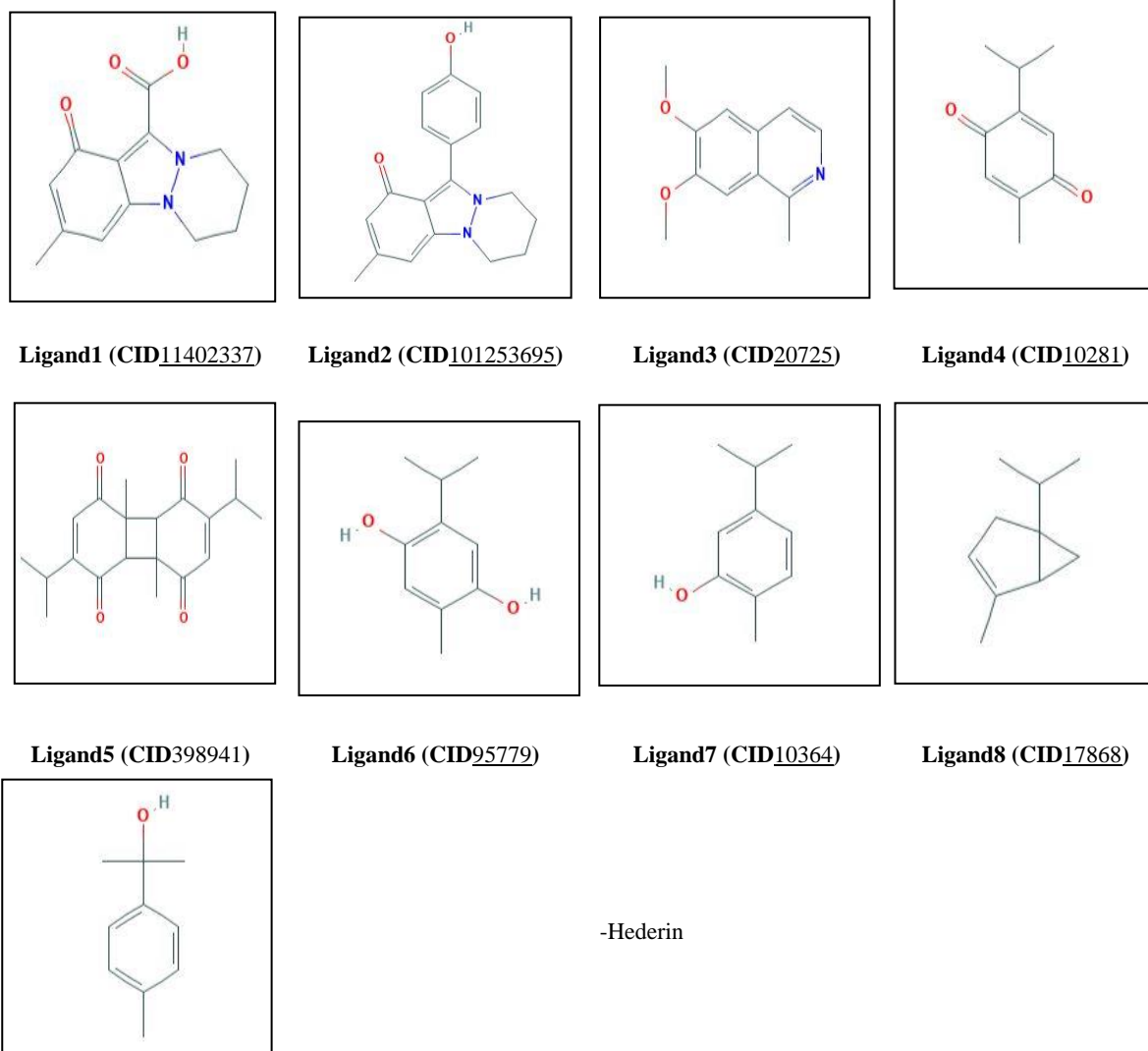
Molecular Dynamics (MD) Simulation

Molecular simulation and molecular modeling techniques are profitably employed nowadays in several industrial sectors. The use of molecular simulation includes, for instance, the design of new molecules or phases through the prediction of their physical or chemical properties. Currently, molecular dynamics (MD) are preferred to become an alternative to experiments to provide transport properties [14, 15].

The best conformer of DPP-4 proteins with ligands was subjected to Molecular Dynamics Simulations MD was performed for both the complex (DPP-4) using the MOE software [5]. MOE dynamics simulation uses the Nosé-Poincaré Andersen (NPA) equations of motion [16, 17]. The Berendsen method was used to adjust and control the temperature each picoseconds [18]. The coordinates were stored every 0.2 ps to get an accurate view of molecular movement. In all simulations the van der Waals cut-out distance was set to 8Å The interactions of the system's amino acids were defined using the NPA algorithm and MMFF94x force field. The default protocols and steps of the MD were used to optimize the system's equilibrium for 100 ps and the production run in 600 ps.

We used MD simulation for each ligand-protein complex to evaluate the interactions' stability for each docking pose. Here, we have shown the detailed analysis of MD simulation results of only three compounds (Lref, L3, L5) with target DPP-4 (See Fig.3, 4, and 5 for supplementary information) because these compounds show better binding affinity for both receptors. To identify the potential of these compounds, molecular dynamics studies were performed using MOE. In the end and according to the molecular dynamics simulation analysis among these 3 compounds the most active compounds were L3 and L5 in DPP-4 proteins.

Table 2: Natural inhibitors of Nigella used for Dipeptidyl peptidase-4 (DPP-4) Enzyme



Ligand9 (CID) 14529

Figure 2 shows the enzyme's active site with a molecule of co-crystallization. The enzyme's active sites with co-crystallization molecule are shown in Table 2. The ligands' minimized toxicity and energy obtained by MOE software are shown in Table 3.

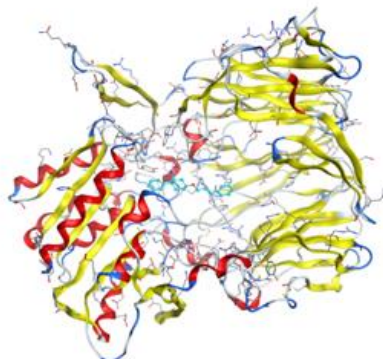


Figure 1. Simplified model of (DPP-4)

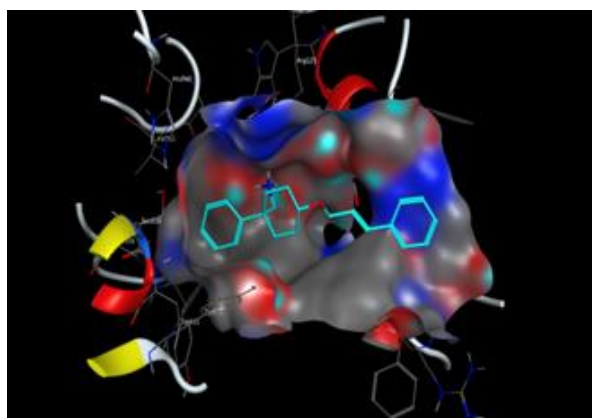


Figure 2. The active site of the isolated enzyme *isolated*

Table 3: Minimization energy of molecules natural For Anti-diabetic action (Kcal/mol)

A /Ligand	Molecules	Energies(Kcal/mol)	LogP	LogS	Toxicity
1	Nigellicine	8.03966e+001	-0.27	-2.45	No
2	Nigellidine	1.01257e+002	2.94	-3.71	No
3	Nigellimine	5.98134e+001	2.56	-2.42	No
4	Thymoquinone	1.59109e+001	1.67	-2.48	No
5	Dithymoquinone	3.74537e+001	2.71	-3.90	No
6	Thymohydroquinone	2.32472e+001	2.53	-2.01	No
7	Carvacrol	2.31484e+001	2.85	-2.69	No
8	alpha- Thujen	2.52974e+001	3.00	-3.44	No
9	p-Cymen	3.18855e+001	2.53	-2.28	No

These ligands are capable of providing crucial biological activities in accordance with the principle of Lipinski, *et al.* (1997) [12].

ADME Properties

Precise characterization and deep understanding of absorption, distribution, metabolism, and elimination (ADME) features of a candidate drug have been well identified as an important element in a small molecule drug discovery and development [19, 20]. The primary cause of failure during the drug development phase is poor pharmacokinetics (PK) and toxicity rather than poor efficacy of the candidate compound. In particular, PK has been the main source of failure in drug development [21, 22]. Lipinski's rule of five [23], Veber's rule [24] Egan's rule [25] and Polar surface area (TPSA), number of rotatable bonds (n-

ROTB) and molecular volume (MV) were calculated using Swiss ADME online property calculation [26] from all parameters for the top-scoring lead compounds.

Results and Discussion

Molecular Docking

We note that the result obtained (Table 1), out of the 9 compounds studied, Dithymoquinone (Fig 1) was predicted to be the strongest DPP-4 enzyme binder that forms a complex with the most stability (Fig 3 and 4) with the lowest energy (-6.21730804 Kcal/mol) and only Van der Waals interactions are perceptible in complex formed with Dithymoquinone and the existence of two electric force, DPP-4 GLU205, GLU206 (H-donor, ionic) at distances of 2.61 and 2.37Å, respectively. This suggests that Dithymoquinone can inhibit DPP-4 enzyme. The second best binder is Nigellimine with the energy of -5.61848545 Kcal/mol that interacts with a single amino acid [SER630 H- π at a distance of 4.1 Å weak interaction, with the existence of two electric force GLU205, GLU206 (H-donor, ionic) at the distance of 2.61, 2.37Å respectively, suggesting that Nigellimine can inhibit DPP-4 enzyme and interfere with [SER630(Å) H- π].

Table 4: Energy balance of complexes formed with DPP-4 without water molecules (Kcal/mol).

Mol	score	Rmsd-refine	E-Conf	E-PLACE	E-SCORE1	E-REFINE	E-SCORE2
Complexe-1	-4.881	3.082	11.488	-62.956	-10.950	-17.035	-4.881
Complexe-2	-4.881	3.083	11.489	-62.956	-10.950	-17.030	-4.881
Complexe-3	-5.618	0.908	91.712	-69.999	-10.528	-15.856	-5.618
Complexe-4	-4.715	2.153	-5.008	-58.264	-8.829	-12.904	-4.715
Complexe-5	-6.217	1.390	-3.570	-85.910	-10.950	-4.197	-6.217
Complexe-6	-4.743	2.221	-4.188	-61.507	-11.926	-13.897	-4.743
Complexe-7	-4.422	1.989	9.381	-65.491	-10.764	-14.735	-4.422
Complexe-8	-3.988	2.6769	29.242	-36.862	-6.576	-9.982	-3.988
Complexe-9	-4.222	1.655	26.157	-40.427	-8.603	-12.375	-4.222

Table 5: Energy balance of complexes formed with DPP-4 with water molecules (Kcal/mol).

Mol	score	Rmsd-refine	E-Conf	E-PLACE	E-SCORE1	E-REFINE	E-SCORE2
Complexe-1	-6.103	1.113	12.906	-58.568	-12.377	-11.092	-6.103
Complexe-2	-5.900	0.838	103.693	-41.983	-13.273	6.640	-5.900
Complexe-3	-6.143	0.985	53.193	-72.814	-12.816	-8.541	-6.043
Complexe-4	-5.904	1.269	-2.561	-51.773	-9.005	-6.589	-5.904
Complexe-5	-8.323	1.503	-10.176	-46.872	-12.600	-6.540	-8.323
Complexe-6	-5.121	1.486	-4.795	-59.826	-14.246	-12.035	-5.121
Complexe-7	-4.900	0.593	10.675	-45.550	-12.991	0.196	-4.900
Complexe-8	-5.385	2.258	32.309	-34.787	-7.365	-8.456	-5.385
Complexe-9	-5.757	0.904	26.703	-64.950	-9.108	-10.524	-5.757

S: The final score; is the last step's score. **rmsd_refine:** The mean square deviation between the laying before refinement and after refinement poses.

E_conf: Energy conformer. **E_place:** Score of the placement phase. **E_scor1:** Score of the first step of notation. **E_refine:** Score of the refinement step and the number of conformations generated by ligand. **E_scor2:** Score of the first step notation, number of poses: Number of conformations.

Table 6: Results of bonds between atoms of compounds and residues of the active site

Compounds	S-score (kcal/mol)	Bonds between atoms of compounds and residues of the active site					
		Atom of compound	Involved receptor atoms	Involved receptor residues	Type of interaction bond	Distances (Å)	Energies (kcal/mol)
L1	-6.103	O1	O	HOH 0	H-Acceptor	3.26	-0.9
		O2	NH1	ARG125	H-Acceptor	3.38	-0.7
		O3	NH2	His740	Ionic	4.00	-0.5
L2	-5.900	O2	O	HOH 0	H-Acceptor	3.23	-0.9
		O2	O	HOH 0	H-Acceptor	3.40	-1.0
L3	-6.143	6-ring	CB	TYR631	pi-H	4.62	0.9
L4	-5.904	/	/	/	/	/	/
L5	-8.323	C21	6-ring	TYR662	H-pi	4.62	-0.7
L6	-5.121	O1	OE1	GLU206	H-donor	3.34	-1.9
L7	-4.900	/	/	/	/	/	/
L8	-5.385	/	/	/	/	/	/
L9	-5.757	/	/	/	/	/	/

Molecular Dynamics

Thermodynamic properties

Using the MD simulation approach, we have studied the evolution thermodynamic properties of the ligand of reference, complex 5 and complex 14 in NVT ensemble (See Table 7).

Table 7: Thermodynamic properties calculated in reel units. Pressure $P = P^* \epsilon / \sigma^3$, Energy of configuration $U = U^* N \epsilon$, translation Kinetic Energy $EKT = EKT^* N \epsilon$ and Enthalpy $H = H^* N \epsilon$.

Stage	Method	H	U	EKT	P	V	T
SP ₁	NVT Complex_5	0.421028107	8401.52051	8740.75977	-132.770828	94995.6406	298.051544
	NVT Complex_3	-0.831780791	8596.08301	8809.4082	121.921898	94855.6484	300.891937
	NVT Complex_5	2.43320942	7869.79102	8687.17969	-31.0936623	94995.6406	296.224518
	NVT Complex_3	-0.660606146	8178.89014	8570.6543	-4.58998823	94855.6484	292.737122
	NVT Complex_5	2.355932	7814.8999	8675.27539	91.1705246	94995.6406	295.818604
	NVT Complex_3	-0.953255355	8088.30225	8675.26074	13.7283316	94855.6484	296.310028
SP ₂	NVT Complex_5	0.694466531	7757.69238	8653.01367	39.948761	94995.6406	295.059509
	NVT Complex_3	3.3615315	7998.1958	8531.42188	-52.9334373	94855.6484	291.397095
	NVT Complex_5	-0.884586275	-0.884586275	8610.75293	-168.186905	94995.6406	293.618439
	NVT Complex_3	0.730786264	7968.19922	8624.98633	39.8331184	94855.6484	294.592865
	NVT Complex_5	6.42101383	7849.32715	8554.99512	-125.444656	94995.6406	291.717163
	NVT Complex_3	2.99717617	7971.15918	8635.4248	-34.5075188	94855.6484	294.949402
SP ₃	NVT Complex_5	3.24411488	7658.03027	8572.21191	12.3245678	94995.6406	292.304199
	NVT Complex_3	-0.839430809	7778.39307	8716.44922	63.0960693	94855.6484	297.716858
	NVT Complex_5	3.96593213	7642.80664	8640.72168	-125.374969	94995.6406	294.64035
	NVT Complex_3	0.0389520749	7824.72363	8543.41992	3.41107082	94855.6484	291.806885
	NVT Complex_5	6.874156	7640.20361	8786.30957	-37.6744232	94995.6406	299.604736
	NVT Complex_3	-2.41168928	7649.59961	8607.6582	-133.50444	94855.6484	294.001007

The complex Lig3 has very important configuration energy. This system gives values far more important for thermodynamic properties. This may be explained by the complexity of the molecule that leads to changes in the 3D structure of the system to the vibrational and rotational level. These results are in agreement with the docking prediction results (Tables 5).

Prediction of the Relative global softness

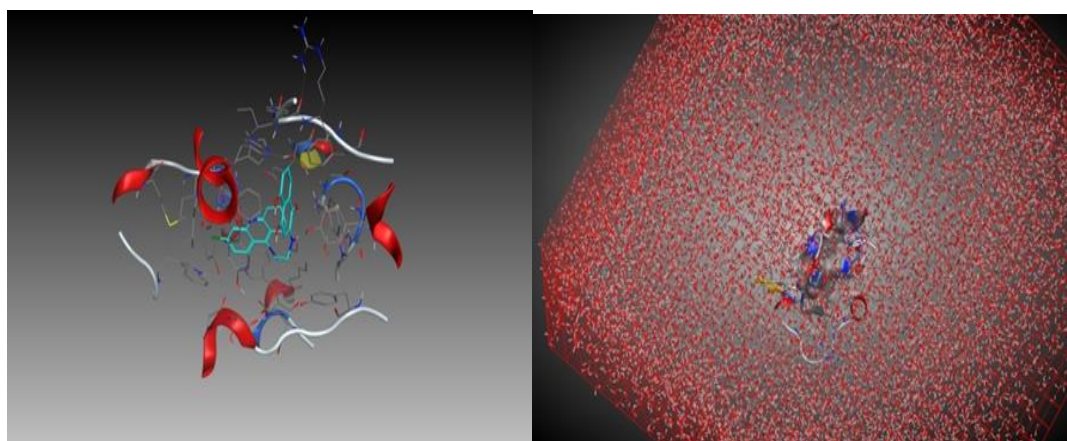
The relative interaction scores (Docking results) of Ligref, Lig5, and Lig3 (see Table 4) in the inhibition were rationalized using the global softness S index. The numerical values of this quantity are given in Table 8.

Table 8: LUMO and HOMO energies, and global reactivity indices μ , η , ω for Ligref, Lig 3, and Lig 5 at the B3LYP/6-311g(d,p)

Compound	HOMO (au)	LUMO (au)	μ (au)	η (au)	S (au ⁻¹)
Lig ref	-0.1254	-0.0125	-0.2415	0.2541	3.2544
Lig 3	-0.2542	-0.0452	-0.1254	0.3521	5.2536
Lig 5	-0.2145	-0.3580	-0.1425	0.3015	6.0253

The global softness decreases from Lig5 succeeded by Lig3 and the last one is Lig: ref indicating that Lig5 is the softest molecule of this series, $S = 6.0253\text{eV}$. Therefore, Lig5 is predicted to be the most interactive system followed by Lig3 $S = 5.2536\text{eV}$ and while Ligref: $S = 3.2544\text{eV}$ will obviously be the less soft one. These results are in total agreement with the Docking prediction results (see Tables 4-5).

When water is included, the best inhibition to the evolution of the pathology studied (type 2 diabetes) is provided. The behavior of water molecules in direct contact with the solute is very important and therefore, it is crucial to ensure that not only the solute but also the first solvation layers are surrounded by a sufficient number of water molecules to ensure the realistic behavior of all the molecules of solvent (Figures 3-4). Refinements of certain terms of the force field describing the water molecule are imperative to ensure good results. For example, the explicit treatment of the electronic polarizability of water molecules can be included as an additional term in an empirical force field. The presence of water is sometimes paramount to ensure a relay between the ligand and the active site [19].

**Figure 5.** Solvation Ligand–Substrate in cube.

In silico assessment of the ADME properties and drug-likeness

A computational study of two top-scoring lead compounds was performed for the assessment of ADME properties and Table 9 shows the obtained values.

Table 9: ADME properties for two top-scoring lead compounds

Entry	ABS	TPSA (Å ²)	n-ROTB	MW	MLog P	n-ON acceptors	n-OHNDH donors	Lipinski's violations	Veber violations	Egan violations
Rule	-	-	-	<500	≤5	<10	<5	≤1	≤1	≤1
L3	High	31.35	2	203.24	1.18	3	0	0	0	0
L5	High	68.28	2	328.40	1.74	4	0	0	0	0

ABS: absorption, TPSA: topological polar surface area, n-ROTB: number of rotatable bonds, MW: molecular weight, MLogP: logarithm of partition coefficient of the compound between water and n-octanol: n-OHNDH donors: number of hydrogen bonds donors, n-ON acceptors: number of hydrogen bond acceptors.

The results showed that compound L3 and compound L5 have high absorptions. In addition, we can note that these compounds comply with Lipinski's rule of 5, Veber's rule, and Egan's rule. where log values ranged between 1.96 – 4.99 (<5), MW range of 292–478 (<500), HBA range of 4-7 (≤ 10) and HBD range of 0-1 (<5), showing that the compounds cannot cause problems with oral bioavailability and thus showing possible utility of both compounds for developing the compound with good drug-like properties.

Conclusion

In this investigation, the inhibition of DPP-4 enzyme was theoretically examined by molecular docking analyses MD simulations. Our calculations showed that the natural inhibitor – Dithymoquinone inhibitor– 5 of the essential oil of *Nigella Sativa* provides more optimized inhibition of Dipeptidyl peptidase-4 for T2DM treatment. These interactions between Dipeptidyl peptidase-4 and those inhibitors are undergoing different interactions between H-acceptors and ionic of natural ones. However, the docking simulation results are optimized under dynamic conditions by MD simulations to prove the stability of the interaction between both proteins and each ligand. Although compounds L3 and L5 have binding affinity with DDP-4 protein in the docking simulation, the ligand-protein interactions mentioned in docking simulation are almost stable in dynamic conditions. These results allow us to propose a natural and reliable treatment during the first stage of T2DM.

References

1. Ferdous AJ, Islam SN, Ahsan M, Hasan CM, Ahmed ZU. In vitro antibacterial activity of the volatile oil of *Nigella sativa* seeds against multiple drug-resistant isolates of *Shigella* spp. and isolates of *Vibrio cholerae* and *Escherichia coli*. *Phytotherapy Research*. 1992 May;6(3):137-40.
2. David RW, Omar AG, Peter AC. The in vitro antitumor activity of some crude and purified components of black seed (*Nigella sativa*). *Anticancer Res*. 1998;18:1527-32.
3. Houghton PJ, Zarka R, de las Heras B, Hoult JR. Fixed oil of *Nigella sativa* and derived thymoquinone inhibit eicosanoid generation in leukocytes and membrane lipid peroxidation. *Planta medica*. 1995 Feb;61(01):33-6.
4. Khanna T, Zaidi FA, Dandiya PC. CNS and analgesic studies on *Nigella sativa*. *FITOTERAPIA-MILANO*. 1993;64:407-.
5. Al-Hader A, Aqel M, Hasan Z. Hypoglycemic effects of the volatile oil of *Nigella sativa* seeds. *International journal of pharmacognosy*. 1993 Jan 1;31(2):96-100.
6. Parr RG, Donnelly RA, Levy M, Palke WE. Electronegativity: the density functional viewpoint. *The Journal of Chemical Physics*. 1978 Apr 15;68(8):3801-7.
7. Senet P. Chemical hardnesses of atoms and molecules from frontier orbitals. *Chemical physics letters*. 1997 Sep 5;275(5-6):527-32.
8. CCGI M. Molecular Operating Environment (MOE), 2013.08. Chemical Computing Group Inc., Montreal. 2016.
9. Parr RG, Pearson RG. Absolute hardness: companion parameter to absolute electronegativity. *Journal of the American Chemical Society*. 1983 Dec;105(26):7512-6.
10. Koopmans T. Ordering of wave functions and eigenenergies to the individual electrons of an atom. *Physica*. 1933;1:104-13.
11. Lee C, Yang W, Parr RG. Development of the Colle-Salvetti correlation-energy formula into a functional of the electron density. *Physical review B*. 1988 Jan 15;37(2):785.
12. Petersson A, Bennett A, Tensfeldt TG, Al-Laham MA, Shirley WA, Mantzaris J. A complete basis set model chemistry. I. The total energies of closed-shell atoms and hydrides of the first-row elements. *The Journal of chemical physics*. 1988 Aug 15;89(4):2193-218.
13. Frisch MJ, Trucks GW, Schlegel HB, Scuseria GE, Robb MA, Cheeseman JR, Scalmani G, Barone V, Mennucci B, Petersson G, Nakatsuji H. Gaussian 09, revision a. 02, gaussian. Inc., Wallingford, CT. 2009 Jun 11;200:28.
14. Morriss GP, Davis PJ, Evans DJ. The rheology of n alkanes: Decane and eicosane. *The Journal of chemical physics*. 1991 Jun 1;94(11):7420-33.
15. Padilla P, Toxvaerd SR. Fluid n-decane undergoing planar Couette flow. *The Journal of chemical physics*. 1992 Nov 15;97(10):7687-94.
16. Bond SD, Leimkuhler BJ, Laird BB. The Nosé–Poincaré method for constant temperature molecular dynamics. *Journal of Computational Physics*. 1999 May 1;151(1):114-34.
17. Sturgeon JB, Laird BB. Symplectic algorithm for constant-pressure molecular dynamics using a Nosé–Poincaré thermostat. *The Journal of Chemical Physics*. 2000 Feb 22;112(8):3474-82.
18. Berendsen HJ, Postma JV, van Gunsteren WF, DiNola AR, Haak JR. Molecular dynamics with coupling to an external bath. *The Journal of chemical physics*. 1984 Oct 15;81(8):3684-90.
19. Klebe G. Virtual ligand screening: strategies, perspectives and limitations. *Drug discovery today*. 2006 Jul 1;11(13-14):580-94.
20. Prueksaritanont T, Tang C. ADME of biologics—what have we learned from small molecules? *The AAPS journal*. 2012 Sep 1;14(3):410-9.
21. Cheng F, Li W, Liu G, Tang Y. In silico ADMET prediction: recent advances, current challenges and future trends. *Current topics in medicinal chemistry*. 2013 Jun 1;13(11):1273-89.
22. Kacprzyk J, Pedrycz W, editors. *Springer handbook of computational intelligence*. Springer; 2015 May 28.

23. Lipinski CA, Lombardo F, Dominy BW, Feeney PJ. Experimental and computational approaches to estimate solubility and permeability in drug discovery and development settings. *Advanced drug delivery reviews*. 1997 Jan 15;23(1-3):3-25.
24. Veber DF, Johnson SR, Cheng HY, Smith BR, Ward KW, Kopple KD. Molecular properties that influence the oral bioavailability of drug candidates. *Journal of medicinal chemistry*. 2002 Jun 6;45(12):2615-23.
25. Egan WJ, Merz KM, Baldwin JJ. Prediction of drug absorption using multivariate statistics. *Journal of medicinal chemistry*. 2000 Oct 19;43(21):3867-77.
26. Daina A, Michielin O, Zoete V. SwissADME: a free web tool to evaluate pharmacokinetics, drug-likeness and medicinal chemistry friendliness of small molecules. *Scientific reports*. 2017 Mar 3;7:42717.